

## Angular Distributions for Double Ionization of $\text{Li}^-$ by an Ultrashort, Intense Laser Pulse

G. Lagmago Kamta and Anthony F. Starace

*Department of Physics and Astronomy, The University of Nebraska, 116 Brace Laboratory, Lincoln, Nebraska 68588-0111*  
(Received 20 September 2000)

We predict photoelectron angular distributions for double ionization of  $\text{Li}^-$  by both weak and intense ultrashort, linearly polarized laser pulses by direct numerical integration of the three-dimensional, time-dependent Schrödinger equation.  $\text{Li}^-$  is treated as a two-active electron system. Near threshold, for low intensity we recover general features of angular distributions for one-photon double ionization. For the intense field (multiphoton) case, the photoelectron angular distribution changes significantly, particularly in directions parallel and perpendicular to the laser polarization axis.

DOI: 10.1103/PhysRevLett.86.5687

PACS numbers: 32.80.Rm, 31.70.Hq, 32.80.Gc, 32.80.Wr

Double photoionization remains a challenge in atomic physics due to the difficulty of describing the correlated motion of two interacting continuum electrons in the field of an ion core. The simplest case of single-photon double ionization is still the object of much research [1]. Most theories for this case evaluate triply differential cross sections (TDCS) in terms of transition matrix elements coupling initial and final states. While methods exist to obtain the initial state to arbitrary accuracy, the search for analytic representations for the asymptotic final state wave function continues [2]. Many *ab initio* approaches use the stationary Schrödinger equation to construct the final state numerically [1,3]. Direct numerical integration of the three-dimensional, time-dependent Schrödinger equation (TDSE) is the only approach adequate for studying the interaction of an atomic system with an ultrashort, intense laser pulse. For two-electron systems, this remains a challenging task. However, recent increases in both computer speeds and data storage capacities has allowed theorists to begin tackling this problem without gross approximations. Several approaches that account for the pulse shape have been developed [4,5]. For double ionization by intense fields, very little is known concerning the distribution of ejected electrons, despite recent electron coincidence [6] and COLTRIMS [7] measurements. On the theoretical side, although angle-averaged radial probability density plots (averaged over all angles except  $\theta_{12}$ ) indicate that the two electrons may be ejected with a small relative angle  $\theta_{12}$  by an ultrashort intense laser pulse [8], an approach providing detailed and complete angular distributions is still needed. For this purpose, one requires a nonperturbative approach that includes correlation effects not only in the initial state but also in the time-dependent final state throughout the interaction time of the system with the laser field. We describe such an approach that involves the solution of the TDSE for a real two-active electron system and present angular distributions following one-photon and multiphoton double ionization of  $\text{Li}^-$ .

For approaches that integrate the TDSE on a finite radial grid, there is no precise definition for the double ionization probability (DIP) because of the difficulty of desen-

tangling single and double ionization contributions in the time-propagated wave function. The DIP (including both sequential and nonsequential) is usually defined as [9]

$$P = \int d\Omega_1 \int d\Omega_2 \int_{r_1 > r_c} dr_1 \int_{r_2 > r_c} dr_2 |\Psi(\mathbf{r}_1, \mathbf{r}_2, T)|^2, \quad (1)$$

where  $\mathbf{r}_j \equiv (r_j, \theta_j, \phi_j)$  and  $d\Omega_j \equiv \sin\theta_j d\theta_j d\phi_j$  ( $j = 1, 2$ ) denote, respectively, the coordinates and the differential solid angles for the two electrons.  $\Psi(\mathbf{r}_1, \mathbf{r}_2, T)$  represents the antisymmetrized wave function at time  $T$ , the end of the laser pulse. In Eq. (1), angular integrations are performed over all angles (i.e.,  $0 \leq \theta_j \leq \pi$ ,  $0 \leq \phi_j \leq 2\pi$ ), while radial integrations involve only configurations where the two electrons are both at distances larger than a cutoff radius  $r_c$ , which is chosen so that most of the ground state probability distribution lies within  $0 \leq r_1, r_2 \leq r_c$ . The DIP defined by (1) is inexact because the residual ground and the doubly excited state populations may contribute to the region  $r_c \leq r_1, r_2 \leq \infty$ . These contributions may be small but nevertheless not negligible compared to the DIP, which is small as well. We also define the DIP by (1), but with the difference that in  $\Psi(\mathbf{r}_1, \mathbf{r}_2, T)$  we exclude contributions from bound and doubly excited states. To obtain the electron angular distributions for double ionization, we omit integration over the solid angles in (1), so that

$$\frac{d^2P}{d\Omega_1 d\Omega_2} = \int_{r_1 > r_c} dr_1 \int_{r_2 > r_c} dr_2 |\Psi(\mathbf{r}_1, \mathbf{r}_2, T)|^2 \quad (2)$$

represents a *doubly differential double ionization probability* (DDDIP) for electron 1 to emerge in the solid angle  $d\Omega_1$  and electron 2 within  $d\Omega_2$ . The DDDIP is a function of the four angles  $\theta_1, \phi_1, \theta_2,$  and  $\phi_2$ ; also, it is not differential in energy and therefore accounts for all possible energy transfers to the electrons from the laser field pulse as well as for all possible energy sharings among the two ejected electrons. As in [10], this approach avoids the need to specify asymptotic boundary conditions. In this paper, atomic units are used and angles are expressed in radians, unless otherwise stated.

In solving the TDSE we treat the  $\text{Li}^-$  ion as a two-active electron system, with each electron moving in the field of a potential  $V(r)$  describing the  $\text{Li}^+$  core [11,12]. This potential accounts for the polarizability of the  $\text{Li}^+$  core and contains semiempirical parameters which are fitted to reproduce the experimentally measured energy levels of Li. It has been used successfully in time-independent photodetachment calculations for  $\text{Li}^-$  whose results agree well with experiment in the perturbative regime [12,13].

The TDSE for the atomic system interacting with a linearly polarized laser field is  $i \frac{\partial}{\partial t} \Psi(\mathbf{r}_1, \mathbf{r}_2, t) = [H_0 + D(t)]\Psi(\mathbf{r}_1, \mathbf{r}_2, t)$ . Here  $H_0 = h(r_1) + h(r_2) + \frac{1}{r_{12}}$  is the atomic Hamiltonian, which includes the correlation term, and  $h(r) = -\Delta/2 + V(r)$  is the one-electron Hamiltonian for the interaction of each active electron with the  $\text{Li}^+$  core.  $D(t) = \mathbf{A}(t) \cdot (\mathbf{p}_1 + \mathbf{p}_2)$  is the (velocity form) dipole operator for the interaction of the system with the laser field, where  $\mathbf{A}(t) = \mathbf{z}A_0 f(t) \sin \omega t$  is the vector potential,  $\omega$  is the laser frequency,  $\mathbf{z}$  is the polarization unit vector, and  $f(t)$  is a squared cosine envelope.

We solve the TDSE in a box by expanding the wave function  $\Psi(t)$  in a basis as follows:

$$\Psi(\mathbf{r}_1, \mathbf{r}_2, t) = \sum_{L,M} \sum_{\ell_1, \ell_2} \sum_{n_1, n_2} \psi_{n_1 n_2}^{\ell_1 \ell_2 LM}(t) \times \mathcal{A} \frac{R_{n_1, \ell_1}(r_1)}{r_1} \frac{R_{n_2, \ell_2}(r_2)}{r_2} \mathcal{Y}_{\ell_1, \ell_2}^{L,M}(\Omega_1, \Omega_2), \quad (3)$$

where  $\mathcal{A}$  is the antisymmetrization operator. The expansion coefficients are denoted by  $\psi_{n_1 n_2}^{\ell_1 \ell_2 LM}$  and the bipolar spherical harmonics  $\mathcal{Y}_{\ell_1, \ell_2}^{L,M}$  couple the individual angular momenta of the two electrons in  $LS$ -coupling. Because the laser field is linearly polarized and the ground state of  $\text{Li}^-$  has  $^1S$  symmetry, we may set  $M = 0$  in (3). The radial functions  $R_{n, \ell}$  are obtained by solving the one-electron radial Schrödinger equation,  $[-\frac{1}{2} \frac{d^2}{dr^2} + \frac{\ell(\ell+1)}{2r^2} + V(r)]R(r) = ER(r)$ , in a box of size  $r = r_0$  with the boundary conditions  $R_{n, \ell}(r_0) = 0$ . The wave function (3) is subjected to similar boundary conditions:  $\Psi(r_1, r_2 = r_0, t) = \Psi(r_1 = r_0, r_2, t) = 0$ . To minimize flux reflections at the boundaries of the box, its size, the laser intensities, and the pulse duration are adjusted such that the wave function remains negligible at  $r_j = r_0$  ( $j = 1, 2$ ).

Diagonalizing  $H_0$  in the above basis yields a set of discrete two-electron atomic eigenstates (comprising only one bound state for  $\text{Li}^-$ , as well as continuum and other pseudo-states), which permit one to solve the TDSE in a more convenient (atomic) eigenstate representation [4] in which the wave function  $\Phi(t)$  represents a linear combination of the atomic eigenstates with time-dependent coefficients. The resulting set of first-order differential equations in time is solved using an embedded Runge-Kutta method of order 5 [14]. From  $\Phi(T)$  in the atomic eigenstate basis at the end of the pulse excitation, one obtains  $\Psi(T)$  by a matrix-vector product. In obtaining  $\Psi(T)$  for computing the DIP, we set to zero all components of  $\Phi(T)$  cor-

responding to atomic states below the double ionization threshold (DIT), thereby eliminating spurious contributions to the DDDIP from the ground state, doubly excited states, and singly ionized states below the DIT.  $\Psi(T)$  is thus a continuum wave function describing both doubly and singly ionized continua having energies above the DIT. The radial integration in the domain  $r_c \leq r_1, r_2 \leq \infty$  is then used to separate approximately the doubly ionized continua from the remaining singly ionized continua.

We use eight total angular momenta ( $L = 0, 1, 2, 3, 4, 5, 6, \text{ and } 7$ ) and a box size  $r_0 = 250$  a.u. For each  $L$ , 2200 to 3700 configurations are used, leading to a total of about 21 000 ordinary differential equations to be solved. Such a large expansion is necessary to obtain an adequate density of states in the vicinity of the DIT. Typical run times for time propagation are about 24 h on a 660 Mhz DEC EV6 work station. We have varied  $r_0$  from 180 to 300 a.u., as well as the number of angular momenta, to check the stability of our results. The binding energy obtained for  $\text{Li}^-$  is  $E_g = -0.0225$  a.u., which is in agreement with the reference value  $-0.02269$  a.u. [15]. Ejecting the two active electrons in  $\text{Li}^-$  requires an energy of about 0.2205 a.u. (6 eV). We have verified that, for low intensities (up to  $10^{10}$  W/cm $^2$ ), the detachment yield [given by  $1 - P_0$ , where  $P_0$  is the projection of  $\Psi(T)$  on the field-free bound state] depends linearly on the laser peak intensity (on a log-log scale), in agreement with lowest order perturbation theory. A cutoff radius  $r_c = 25$  a.u. is used. (Note that the ground state of  $\text{Li}^-$  extends to approximately 20 a.u.). We varied  $r_c$  between 20 and 25 a.u. and found a 9% maximum difference in the magnitude of the DDDIP, but the angular distribution remains unchanged.

We first treat double ionization by a weak laser pulse of peak intensity  $I = 10^9$  W/cm $^2$ , frequency  $\omega = 0.235$  a.u., and 38 cycles within the full width at half maximum (FWHM) in  $f(t)$  (corresponding to about 24 fs). The low intensity used makes the absorption of a single photon predominant. The frequency chosen is near the DIT (giving about 0.4 eV of excess energy above threshold), where one expects correlation effects to be strong. The number of cycles used is large enough for the pulse to have a relatively narrow energy bandwidth. Indeed, a plot of the probability amplitudes of the wave function with respect to the atomic energies shows a single, well-resolved peak above the DIT, indicating absorption of a single photon. At the end of laser excitation, both the population removed from the ground state and the population above the DIT are almost identically equal to  $1.1 \times 10^{-5}$ . This indicates that one-photon absorption is the dominant process and that most of the population remains in the ground state. Three-dimensional plots of the DDDIP with respect to the polar angles are given in Figs. 1(a) and 1(b) for an emission of the two electrons with azimuthal angles  $(\phi_1 = 0, \phi_2 = 0)$  and  $(\phi_1 = 0, \phi_2 = \pi)$ , respectively. Analysis of both figures allows one to draw the following inferences (which result from the Coulomb repulsion

between the two electrons): (i) The emission of both electrons in opposite directions is higher in magnitude than the emission in the same direction. (ii) The DDDIP is negligible in the vicinity of  $\theta_1 = \theta_2 = 0$  and  $\theta_1 = \theta_2 = \pi$  in both figures as well as in the vicinity of  $\theta_1 \approx \theta_2$  in Fig. 1(a). This indicates that electrons are predominantly emitted at large relative angles. The strong signature of correlation effects in the single-photon double ionization process is better illustrated in Fig. 2, where we plot DDDIP patterns (extracted from Fig. 1) in polar coordinates, for various emission angles  $\theta_1$  of electron 1. Note the node in the DDDIP pattern at angles  $\theta_1 = \theta_2 = \pi/2$  [see Fig. 2(c) and the valley in Fig. 1(b)], indicating that there is no emission of both electrons in the direction perpendicular to the polarization axis. This agrees with a selection rule valid for any sharing of the excess energy [16]. The fact that our DDDIP accounts for all possible energy sharing configurations of the excess energy is illustrated more clearly in Fig. 2(a). Indeed, according to selection rules for the TDCS for equal energy sharing [16], there should be a node at angles  $(\theta_1, \theta_2) = (0, \pi)$  and  $(\theta_1, \theta_2) = (\pi, 0)$ , i.e., the lobe along the polarization axis in Fig. 2(a) should be absent. Here this lobe arises from contributions of unequal energy sharing configurations. Except for this particular situa-

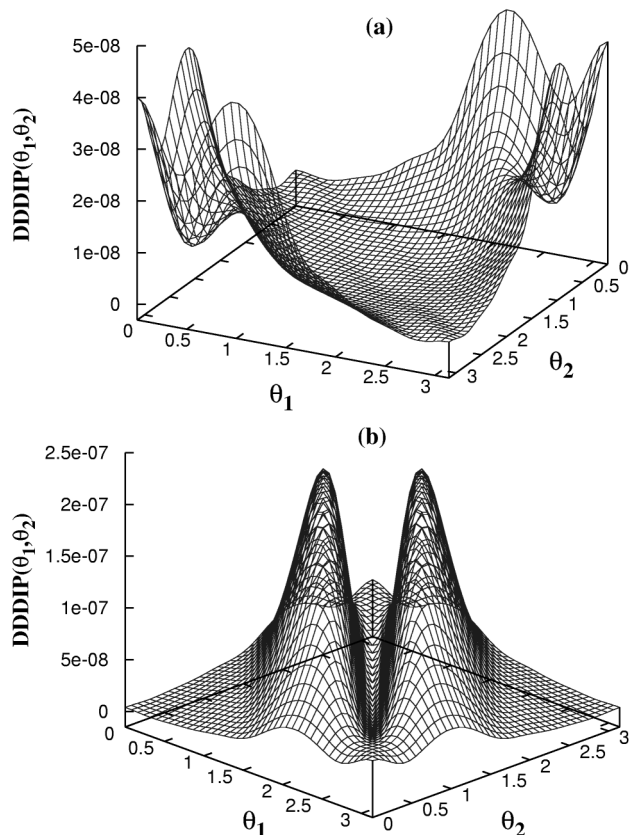


FIG. 1. Single-photon DDDIP for  $\text{Li}^-$  by a weak, linearly polarized laser pulse of peak intensity  $I = 10^9 \text{ W/cm}^2$ , frequency  $\omega = 0.235 \text{ a.u.}$ , and FWHM of 24 fs: (a) for  $\phi_1 = \phi_2 = 0$  and (b) for  $\phi_1 = 0$  and  $\phi_2 = \pi$ . Note that (a) and (b) are shown from different angles.

tion, the angular distributions in Figs. 2(b)–2(d) consist essentially of two lobes whose relative size is a function of the angle between  $\mathbf{k}_1$  and  $\mathbf{z}$ . Similar features have been obtained for He by both perturbative calculations [16] and a “Wannier” analysis [17].

Consider now a laser pulse, of peak intensity  $2 \times 10^{11} \text{ W/cm}^2$ , frequency 0.038 a.u., and 3 cycles at FWHM, corresponding to about 12 fs. At the end of the pulse, more than 75% of the ground state is depleted, indicating that, although the intensity is not too high, we are in the fully nonperturbative regime for  $\text{Li}^-$ . For this frequency at least six photons are necessary to reach the DIT. The DDDIP is presented in Figs. 3(a) and 3(b) for electron emission with azimuthal angles  $(\phi_1 = 0, \phi_2 = 0)$  and  $(\phi_1 = 0, \phi_2 = \pi)$ , respectively. One observes very different angular distributions from those for single-photon double ionization. The DDDIP distribution has four prominent peaks, corresponding to the four possible configurations for ejection of the two electrons along the polarization axis: (i) both along positive  $\mathbf{z}$ , (ii) both along negative  $\mathbf{z}$ , (iii) electron 1 along positive  $\mathbf{z}$  and electron 2 along negative  $\mathbf{z}$ , and (iv) the configuration (iii) with electrons 1 and 2 exchanged. [Note that (iii) and (iv) are identical in magnitude.] That the configurations (i) and (ii), which were not observed at low intensity because of the Coulomb repulsion, are now prominent illustrates the decreasing influence of the Coulomb interaction *vis-à-vis* the laser-atom interaction at high laser intensity. It is also a signature of nonsequential double ionization. However, peaks corresponding to configurations in which electrons are emitted in opposite directions along the polarization axis are more intense. Contrary to the one-photon case, the differences in shape and magnitude between the DDDIP for double ejection with azimuthal angles  $(\phi_1, \phi_2) = (0, 0)$  and  $(0, \pi)$  are now less significant. Major differences between the two configurations appear away from the polarization axis, with a particularly enhanced difference

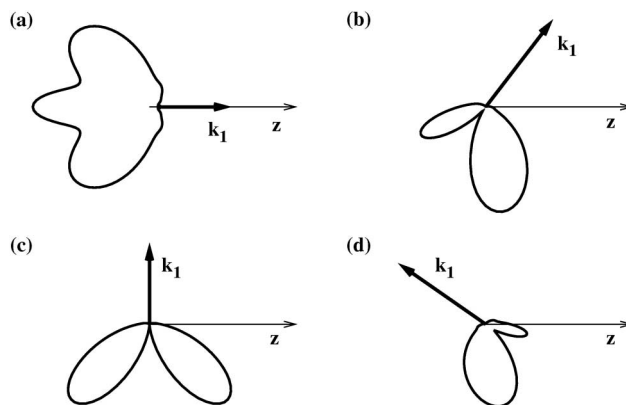


FIG. 2. Single-photon DDDIP patterns in polar coordinates for four emission angles  $\theta_1$  (with directions given by the unit vector  $\mathbf{k}_1$ ) of electron 1: (a)  $\theta_1 = 0$ , (b)  $\theta_1 = \pi/3$ , (c)  $\theta_1 = \pi/2$ , and (d)  $\theta_1 = 3\pi/4$ . Laser parameters are the same as shown in Fig. 1.

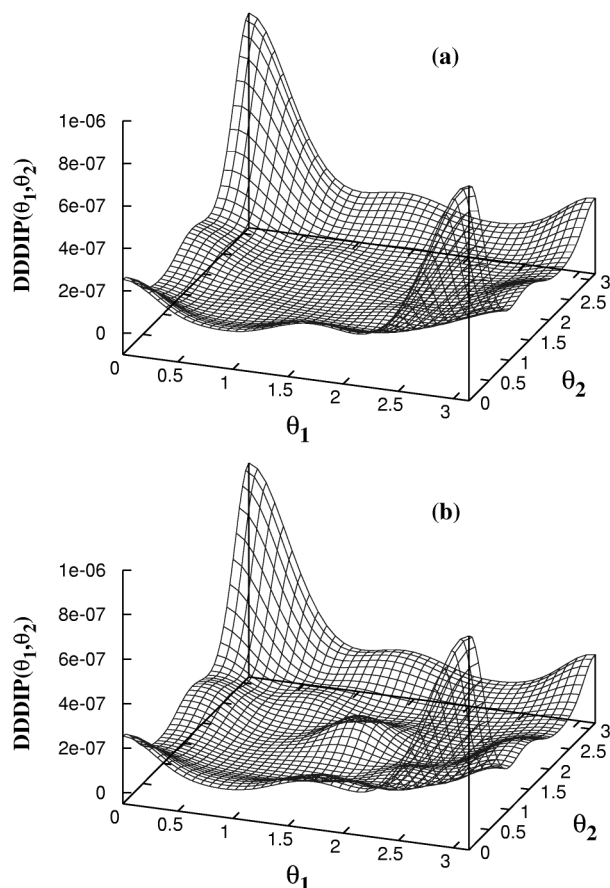


FIG. 3. Multiphoton DDDIP for  $\text{Li}^-$  for an intense laser pulse of peak intensity  $2 \times 10^{11} \text{ W/cm}^2$ ,  $\omega = 0.038 \text{ a.u.}$ , and FWHM of 12 fs: (a) for  $(\phi_1 = 0, \phi_2 = 0)$  and (b) for  $(\phi_1 = 0, \phi_2 = \pi)$ .

at  $\theta_1 = \theta_2 = \pi/2$ . Indeed, due to the contributions of higher order total angular momentum channels in the process, the node observed in the one-photon case at  $\theta_1 = \theta_2 = \pi/2$  disappears. As shown in Fig. 3(b), one observes a strong local maximum at these angles for the  $(\phi_1, \phi_2) = (0, \pi)$  case. In Fig. 3(a), one can barely observe a much smaller maximum for emission of both electrons in the same direction at these angles.

In the one-photon case (Fig. 1), the DIP obtained without removing contributions from states below the DIT is only a few percent higher (in relative value) than the actual one, and the change in angular distributions is also small, but perceptible for the emission at  $\phi_1 = \phi_2 = 0$ : the node expected at  $\theta_1 = \theta_2 = \pi/2$  is replaced by a local maximum, i.e., a distinctive bump appears where Fig. 1(a) shows a valley. However, in the multiphoton case (Fig. 3), where intermediate photon resonances lie below the DIT, the consequence of not removing spurious contributions is dramatic: the DIP obtained in this case is more than 10 times higher than our results.

We have presented a nonperturbative approach for obtaining angular distributions in the one-photon and

multiphoton cases for double ionization by an ultrashort, linearly polarized laser pulse, based on direct numerical integration of the three-dimensional TDSE. Our results show that the electron Coulomb repulsion and other selection rules strongly affect the emission angles of the two electrons in the one-photon double ionization process. In the multiphoton case, electrons may possibly be ejected in all directions, but with sharp peaks along the directions parallel and perpendicular to the polarization axis of the field. For the intensities studied, configurations where electrons are ejected in opposite directions are more likely than those for ejection in the same direction.

We thank Chien-Nan Liu and Bernard Piroux for fruitful discussions. This work was supported by the Dept. of Energy, BES, Div. Chem. Sciences, under Grant No. DE-FG03-96ER14646.

- [1] J. S. Briggs and V. Schmidt, *J. Phys. B* **33**, R1 (2000); G. C. King and L. Avaldi, *J. Phys. B* **33**, R215 (2000).
- [2] A. Engels *et al.*, *J. Phys. B* **30**, L811 (1997).
- [3] J. T. Broad and W. P. Reinhart, *Phys. Rev. A* **14**, 2159 (1976); D. Proulx and R. Shakeshaft, *Phys. Rev. A* **48**, R875 (1993); A. S. Kheifets and I. Bray, *Phys. Rev. A* **54**, R995 (1996); K. W. Meyer, C. H. Greene, and B. D. Esry, *Phys. Rev. Lett.* **78**, 4902 (1997).
- [4] X. Tang, H. Rudolph, and P. Lambropoulos, *Phys. Rev. A* **44**, R6994 (1991); A. Scrinzi and B. Piroux, *Phys. Rev. A* **58**, 1310 (1998); G. Lagmago Kamta *et al.*, in *Multiphoton Processes*, edited by L. F. DiMauro, R. R. Freeman, and K. C. Kulander (AIP, New York, 2000), p. 219.
- [5] C. A. Nicolaides *et al.*, *J. Phys. B* **29**, 231 (1996); J. Parker *et al.*, *J. Phys. B* **29**, L33 (1996); M. S. Pindzola and F. Robicheaux, *Phys. Rev. A* **57**, 318 (1998);
- [6] B. Witzel *et al.*, *Phys. Rev. Lett.* **85**, 2268 (2000).
- [7] Th. Weber *et al.*, *Phys. Rev. Lett.* **84**, 443 (2000); R. Moshhammer *et al.*, *Phys. Rev. Lett.* **84**, 447 (2000).
- [8] J. S. Parker *et al.*, in *Multiphoton Processes*, edited by L. F. DiMauro, R. R. Freeman, and K. C. Kulander (AIP, New York, 2000), p. 273.
- [9] D. Dundas, K. T. Taylor, J. S. Parker, and E. S. Smyth, *J. Phys. B* **32**, L231 (1999); D. G. Lappas *et al.*, in *Multiphoton Processes*, edited by L. F. DiMauro, R. R. Freeman, and K. C. Kulander (AIP, New York, 2000), p. 245; H. G. Muller, *ibid.*, p. 257; R. Panfili *et al.*, *ibid.*, p. 265.
- [10] C. W. McCurdy and T. N. Rescigno, *Phys. Rev. A* **56**, R4369 (1997).
- [11] F. Robicheaux and C. H. Greene, *Phys. Rev. A* **46**, 3821 (1992).
- [12] C. Pan *et al.*, *Phys. Rev. A* **53**, 840 (1996).
- [13] C. N. Liu and A. F. Starace, *Phys. Rev. A* **58**, 4997 (1998).
- [14] E. Hairer *et al.*, *Solving Ordinary Differential Equations I: Nonstiff Problems* (Springer, Berlin, 1987).
- [15] K. T. Chung and P. Fullbright, *Phys. Scr.* **45**, 445 (1992).
- [16] F. Maulbetsch and J. S. Briggs, *J. Phys. B* **28**, 551 (1995); *ibid.* **26**, L647 (1993).
- [17] A. Huetz *et al.*, *J. Phys. B* **24**, 1917 (1991).